

# Branching Ratio and CP Asymmetry of $B_s \rightarrow K_0^*(1430)\rho(\omega, \phi)$ Decays in the PQCD Approach

Zhi-Qing Zhang \*

*Department of Physics, Henan University of Technology,  
Zhengzhou, Henan 450052, P.R.China*

(Dated: November 26, 2018)

## Abstract

In the two-quark model supposition for  $K_0^*(1430)$ , which can be viewed as either the first excited state (scenario I) or the lowest lying state (scenario II), the branching ratios and the direct CP-violating asymmetries for decays  $\bar{B}_s^0 \rightarrow K_0^{*0}(1430)\phi, K_0^{*0}(1430)\omega, K_0^{*0}(1430)\rho^0, K_0^{*+}(1430)\rho^-$  are studied by employing the perturbative QCD factorization approach. We find the following results: (a) Enhanced by the color allowed tree amplitude with large Wilson coefficients  $a_1 = C_2 + C_1/3$ , the branching ratio of  $\bar{B}_s^0 \rightarrow K_0^{*+}(1430)\rho^-$  is much larger than those of the other three decays and arrives at  $(3.4_{-0.7}^{+0.8}) \times 10^{-5}$  in scenario I, even  $10^{-4}$  order in scenario II, and its direct CP violating asymmetry is the smallest, around 10%, so this channel might be measurable in the current LHC-b experiments, where a large number (about  $10^{12}$ ) of  $B$  mesons will be produced per year. This high statistics will make the measurement possible. (b) For the decay modes  $\bar{B}_s^0 \rightarrow K_0^{*0}(1430)\omega, K_0^{*0}(1430)\rho^0$ , their direct CP-violating asymmetries are large, but it might be difficult to measure them, because their branching ratios are small and less than (or near)  $10^{-6}$  in both scenarios. For example, in scenario I, these values are  $\mathcal{B}(\bar{B}_s^0 \rightarrow K_0^{*0}(1430)\omega) = (8.2_{-1.7}^{+1.8}) \times 10^{-7}, \mathcal{B}(\bar{B}_s^0 \rightarrow K_0^{*0}(1430)\rho^0) = (9.9_{-2.0}^{+2.1}) \times 10^{-7}, \mathcal{A}_{CP}^{dir}(\bar{B}_s^0 \rightarrow K_0^{*0}(1430)\omega) = -24.1_{-2.5}^{+2.8}, \mathcal{A}_{CP}^{dir}(\bar{B}_s^0 \rightarrow K_0^{*0}(1430)\rho^0) = 26.6_{-2.5}^{+2.5}$ . (c) For the decay  $\bar{B}_s^0 \rightarrow K_0^{*0}(1430)\phi$ , the predicted branching ratios are also small and a few times  $10^{-7}$  in both scenarios; there is no tree contribution at the leading order, so its direct CP-violating asymmetry is naturally zero.

PACS numbers: 13.25.Hw, 12.38.Bx, 14.40.Nd

---

\* Electronic address: zhangzhiqing@haut.edu.cn

## I. INTRODUCTION

Along with many scalar mesons found in experiments, more and more efforts have been made to study the scalar meson spectrum theoretically [1–7]. Today, it is still a difficult but interesting topic. Our most important task is to uncover the mysterious structures of the scalar mesons. There are two typical schemes for their classification [1, 2]. Scenario I: the nonet mesons below 1 GeV, including  $f_0(600)$ ,  $f_0(980)$ ,  $K_0^*(800)$ , and  $a_0(980)$ , are usually viewed as the lowest lying  $q\bar{q}$  states, while the nonet ones near 1.5 GeV, including  $f_0(1370)$ ,  $f_0(1500)/f_0(1700)$ ,  $K_0^*(1430)$ , and  $a_0(1450)$ , are suggested as the first excited states. In scenario II, the nonet mesons near 1.5 GeV are treated as  $q\bar{q}$  ground states, while the nonet mesons below 1 GeV are exotic states beyond the quark model, such as four-quark bound states.

In order to uncover the inner structures of these scalar mesons, many factorization approaches are also used to research the  $B$  meson decay modes with a final state scalar meson, such as the generalized factorization approach [8], QCD factorization approach [9–11], and perturbative QCD (PQCD) approach [12–16]. On the experimental side, along with the running of the Large Hadron Collider beauty (LHC-b) experiments, some of  $B_s$  decays with a scalar meson in the final state might be observed in the current [17, 18]. In order to make precise measurements of rare decay rates and CP violating observables in the  $B$ -meson systems, the LHC-b detector is designed to exploit the large number of  $b$ -hadrons produced. LHC-b will produce up to  $10^{12}$   $b\bar{b}$  pairs per year ( $10^7 s$ ). Furthermore, it can reconstruct a  $B$ -decay vertex with very good resolution, which is essential for studying the rapidly oscillating  $B_s$  mesons. In a word,  $B_s$  decays with a scalar in the final state can also serve as an ideal platform to probe the natures of these scalar mesons. So the studies of these decay modes for  $B_s$  are necessary in the next a few years.

Here  $K_0^*(1430)$  can be treated as a  $q\bar{q}$  state in both scenario I and scenario II, it is easy to make quantitative predictions in the two-quark model supposition, so we would like to use the PQCD approach to calculate the branching ratios and the CP-violating asymmetries for decays  $\bar{B}_s^0 \rightarrow K_0^{*0}(1430)\phi$ ,  $K_0^{*0}(1430)\omega$ ,  $K_0^{*0}(1430)\rho^0$ ,  $K_0^{*+}(1430)\rho^-$  in two scenarios. In the following,  $K_0^*(1430)$  is denoted as  $K_0^*$  in some places for convenience. The layout of this paper is as follows. In Sec. II, the decay constants and light-cone distribution amplitudes of relevant mesons are introduced. In Sec. III, we then analyze these decay channels using the PQCD approach. The numerical results and the discussions are given in section IV. The conclusions are presented in the final part.

## II. DECAY CONSTANTS AND DISTRIBUTION AMPLITUDES

In general, the  $B_s$  meson is treated as a heavy-light system, and its Lorentz structure can be written as [19, 20]

$$\Phi_{B_s} = \frac{1}{\sqrt{2N_c}}(\not{P}_{B_s} + M_{B_s})\gamma_5\phi_{B_s}(k_1). \quad (1)$$

The contribution of  $\bar{\phi}_{B_s}$  is numerically small [21] and has been neglected. For the distribution amplitude  $\phi_{B_s}(x, b)$  in Eq.(1), we adopt the following model:

$$\phi_{B_s}(x, b) = N_{B_s} x^2 (1-x)^2 \exp\left[-\frac{M_{B_s}^2 x^2}{2\omega_{b_s}^2} - \frac{1}{2}(\omega_{b_s} b)^2\right], \quad (2)$$

where  $\omega_{b_s}$  is a free parameter, we take  $\omega_{b_s} = 0.5 \pm 0.05$  GeV in numerical calculations, and  $N_{B_s} = 63.67$  is the normalization factor for  $\omega_{b_s} = 0.5$ .

In the two-quark picture, the vector decay constant  $f_{K_0^*}$  and the scalar decay constant  $\bar{f}_{K_0^*}$  for the scalar meson  $K_0^*$  can be defined as

$$\langle K_0^*(p) | \bar{q}_2 \gamma_\mu q_1 | 0 \rangle = f_{K_0^*} p_\mu, \quad (3)$$

$$\langle K_0^*(p) | \bar{q}_2 q_1 | 0 \rangle = m_{K_0^*} \bar{f}_{K_0^*}, \quad (4)$$

where  $m_{K_0^*}(p)$  is the mass (momentum) of the scalar meson  $K_0^*$ . The relation between  $f_{K_0^*}$  and  $\bar{f}_{K_0^*}$  is

$$\frac{m_{K_0^*}}{m_2(\mu) - m_1(\mu)} f_{K_0^*} = \bar{f}_{K_0^*}, \quad (5)$$

where  $m_{1,2}$  are the running current quark masses. For the scalar meson  $K_0^*(1430)$ ,  $f_{K_0^*}$  will get a very small value after the  $SU(3)$  symmetry breaking is considered. The light-cone distribution amplitudes for the scalar meson  $K_0^*(1430)$  can be written as

$$\begin{aligned} \langle K_0^*(p) | \bar{q}_1(z)_l q_2(0)_j | 0 \rangle &= \frac{1}{\sqrt{2N_c}} \int_0^1 dx e^{ixp \cdot z} \\ &\times \{ \not{p} \Phi_{K_0^*}(x) + m_{K_0^*} \Phi_{K_0^*}^S(x) + m_{K_0^*} (\not{n}_+ \not{n}_- - 1) \Phi_{K_0^*}^T(x) \}_{jl}. \end{aligned} \quad (6)$$

Here  $n_+$  and  $n_-$  are lightlike vectors:  $n_+ = (1, 0, 0_T)$ ,  $n_- = (0, 1, 0_T)$ , and  $n_+$  is parallel with the moving direction of the scalar meson. The normalization can be related to the decay constants:

$$\int_0^1 dx \Phi_{K_0^*}(x) = \int_0^1 dx \Phi_{K_0^*}^T(x) = 0, \quad \int_0^1 dx \Phi_{K_0^*}^S(x) = \frac{\bar{f}_{K_0^*}}{2\sqrt{2N_c}}. \quad (7)$$

The twist-2 light-cone distribution amplitude  $\Phi_{K_0^*}$  can be expanded in the Gegenbauer polynomials:

$$\Phi_{K_0^*}(x, \mu) = \frac{\bar{f}_{K_0^*}(\mu)}{2\sqrt{2N_c}} 6x(1-x) \left[ B_0(\mu) + \sum_{m=1}^{\infty} B_m(\mu) C_m^{3/2}(2x-1) \right], \quad (8)$$

where the decay constants and the Gegenbauer moments  $B_1, B_3$  of distribution amplitudes for  $K_0^*(1430)$  have been calculated in the QCD sum rules[10]. These values are all scale dependent and specified below:

$$\text{scenario I} : B_1 = 0.58 \pm 0.07, B_3 = -1.2 \pm 0.08, \bar{f}_{K_0^*} = -(300 \pm 30) \text{ MeV}, \quad (9)$$

$$\text{scenario II} : B_1 = -0.57 \pm 0.13, B_3 = -0.42 \pm 0.22, \bar{f}_{K_0^*} = (445 \pm 50) \text{ MeV}, \quad (10)$$

which are taken by fixing the scale at 1GeV.

As for the twist-3 distribution amplitudes  $\Phi_{K_0^*}^S$  and  $\Phi_{K_0^*}^T$ , we adopt the asymptotic form:

$$\Phi_{K_0^*}^S = \frac{1}{2\sqrt{2N_c}} \bar{f}_{K_0^*}, \quad \Phi_{K_0^*}^T = \frac{1}{2\sqrt{2N_c}} \bar{f}_{K_0^*} (1 - 2x). \quad (11)$$

The distribution amplitudes up to twist-3 of the vector mesons are

$$\langle V(P, \epsilon_L^*) | \bar{q}_{2\beta}(z) q_{1\alpha}(0) | 0 \rangle = \frac{1}{2N_C} \int_0^1 dx e^{ixP \cdot z} [M_V \not{\epsilon}_L^* \Phi_V(x) + \not{\epsilon}_L^* \not{P} \Phi_V^t(x) + M_V \Phi_V^s(x)]_{\alpha\beta}, \quad (12)$$

for longitudinal polarization. The distribution amplitudes can be parametrized as

$$\Phi_V(x) = \frac{2f_V}{\sqrt{2N_C}} [1 + a_2^{\parallel} C_2^{\frac{3}{2}}(2x - 1)], \quad (13)$$

$$\Phi_V^t(x) = \frac{3f_V^T}{2\sqrt{2N_C}} (2x - 1)^2, \quad \phi_V^s(x) = -\frac{3f_V^T}{2\sqrt{2N_C}} (2x - 1), \quad (14)$$

where the decay constant  $f_V$  [22] and the transverse decay constant  $f_V^T$  [23] are given as the following values:

$$f_\rho = 209 \pm 2 \text{ MeV}, f_\omega = 195 \pm 3 \text{ MeV}, f_\phi = 231 \pm 4 \text{ MeV}, \quad (15)$$

$$f_\rho^T = 165 \pm 9 \text{ MeV}, f_\omega^T = 151 \pm 9 \text{ MeV}, f_\phi^T = 186 \pm 9 \text{ MeV}. \quad (16)$$

Here the Gegenbauer polynomial is defined as  $C_2^{\frac{3}{2}}(t) = \frac{3}{2}(5t^2 - 1)$ . For the Gegenbauer moments, we quote the numerical results as [24]:

$$a_{2\rho}^{\parallel} = a_{2\omega}^{\parallel} = 0.15 \pm 0.07, a_{2\phi}^{\parallel} = 0.18 \pm 0.08. \quad (17)$$

### III. THE PERTURBATIVE QCD CALCULATION

Under the two-quark model for the scalar meson  $K_0^*$  supposition, the decay amplitude for  $\bar{B}_s^0 \rightarrow V K_0^*$ , where  $V$  represents  $\rho, \omega, \phi$ , can be conceptually written as the convolution,

$$\mathcal{A}(\bar{B}_s^0 \rightarrow V K_0^*) \sim \int d^4 k_1 d^4 k_2 d^4 k_3 \text{Tr} [C(t) \Phi_{B_s}(k_1) \Phi_V(k_2) \Phi_{K_0^*}(k_3) H(k_1, k_2, k_3, t)], \quad (18)$$

where  $k_i$ 's are momenta of the antiquarks included in each meson, and Tr denotes the trace over Dirac and color indices.  $C(t)$  is the Wilson coefficient which results from the radiative corrections at short distance. In the above convolution,  $C(t)$  includes the harder dynamics at larger scale than the  $M_B$  scale and describes the evolution of local 4-Fermi operators from  $m_W$  (the  $W$  boson mass) down to  $t \sim \mathcal{O}(\sqrt{\bar{\Lambda} M_{B_s}})$  scale, where  $\bar{\Lambda} \equiv M_{B_s} - m_b$ . The function  $H(k_1, k_2, k_3, t)$  describes the four-quark operator and the spectator quark connected by a hard gluon whose  $q^2$  is in the order of  $\bar{\Lambda} M_{B_s}$ , and includes the  $\mathcal{O}(\sqrt{\bar{\Lambda} M_{B_s}})$  hard dynamics. Therefore, this hard part  $H$  can be perturbatively calculated. The functions  $\Phi_{(V, K_0^*)}$  are the wave functions of the vector meson  $V$  and the scalar meson  $K_0^*$ , respectively.

Since the  $b$  quark is rather heavy, we consider the  $B_s$  meson at rest for simplicity. It is convenient to use the light-cone coordinate  $(p^+, p^-, \mathbf{p}_T)$  to describe the meson's momenta,

$$p^\pm = \frac{1}{\sqrt{2}}(p^0 \pm p^3), \quad \text{and} \quad \mathbf{p}_T = (p^1, p^2). \quad (19)$$

Using these coordinates, the  $B_s$  meson and the two final state meson momenta can be written as

$$P_{B_s} = \frac{M_{B_s}}{\sqrt{2}}(1, 1, \mathbf{0}_T), \quad P_2 = \frac{M_{B_s}}{\sqrt{2}}(1 - r_{K_0^*}^2, r_V^2, \mathbf{0}_T), \quad P_3 = \frac{M_{B_s}}{\sqrt{2}}(r_{K_0^*}^2, 1 - r_V^2, \mathbf{0}_T), \quad (20)$$

respectively, where the ratio  $r_{K_0^*(V)} = m_{K_0^*(V)}/M_{B_s}$ , and  $m_{K_0^*(V)}$  is the scalar meson  $K_0^*$  (the vector meson  $V$ ) mass. Putting the antiquark momenta in  $B_s$ ,  $V$ , and  $K_0^*$  mesons as  $k_1$ ,  $k_2$ , and  $k_3$ , respectively, we can choose

$$k_1 = (x_1 P_1^+, 0, \mathbf{k}_{1T}), \quad k_2 = (x_2 P_2^+, 0, \mathbf{k}_{2T}), \quad k_3 = (0, x_3 P_3^-, \mathbf{k}_{3T}). \quad (21)$$

For these considered decay channels, the integration over  $k_1^-$ ,  $k_2^-$ , and  $k_3^+$  in Eq.(18) will lead to

$$\mathcal{A}(B_s \rightarrow V K_0^*) \sim \int dx_1 dx_2 dx_3 b_1 db_1 b_2 db_2 b_3 db_3 \cdot \text{Tr} [C(t) \Phi_{B_s}(x_1, b_1) \Phi_V(x_2, b_2) \Phi_{K_0^*}(x_3, b_3) H(x_i, b_i, t) S_t(x_i) e^{-S(t)}], \quad (22)$$

where  $b_i$  is the conjugate space coordinate of  $k_{iT}$ , and  $t$  is the largest energy scale in function  $H(x_i, b_i, t)$ . In order to smear the end-point singularity on  $x_i$ , the jet function  $S_t(x)$  [25], which comes from the resummation of the double logarithms  $\ln^2 x_i$ , is used. The last term  $e^{-S(t)}$  in Eq.(22) is the Sudakov form factor which suppresses the soft dynamics effectively [26].

For the considered decays, the related weak effective Hamiltonian  $\mathcal{H}_{eff}$  can be written as [27]

$$\mathcal{H}_{eff} = \frac{G_F}{\sqrt{2}} \left[ \sum_{p=u,c} V_{pb} V_{pd}^* (C_1(\mu) O_1^p(\mu) + C_2(\mu) O_2^p(\mu)) - V_{tb} V_{td}^* \sum_{i=3}^{10} C_i(\mu) O_i(\mu) \right]. \quad (23)$$

Here the Fermi constant  $G_F = 1.16639 \times 10^{-5} \text{GeV}^{-2}$  and the functions  $Q_i (i = 1, \dots, 10)$  are the local four-quark operators. We specify below the operators in  $\mathcal{H}_{eff}$  for  $b \rightarrow d$  transition:

$$\begin{aligned} O_1^u &= \bar{d}_\alpha \gamma^\mu L u_\beta \cdot \bar{u}_\beta \gamma_\mu L b_\alpha, & O_2^u &= \bar{d}_\alpha \gamma^\mu L u_\alpha \cdot \bar{u}_\beta \gamma_\mu L b_\beta, \\ O_3 &= \bar{d}_\alpha \gamma^\mu L b_\alpha \cdot \sum_{q'} \bar{q}'_\beta \gamma_\mu L q'_\beta, & O_4 &= \bar{d}_\alpha \gamma^\mu L b_\beta \cdot \sum_{q'} \bar{q}'_\beta \gamma_\mu L q'_\alpha, \\ O_5 &= \bar{d}_\alpha \gamma^\mu L b_\alpha \cdot \sum_{q'} \bar{q}'_\beta \gamma_\mu R q'_\beta, & O_6 &= \bar{d}_\alpha \gamma^\mu L b_\beta \cdot \sum_{q'} \bar{q}'_\beta \gamma_\mu R q'_\alpha, \\ O_7 &= \frac{3}{2} \bar{d}_\alpha \gamma^\mu L b_\alpha \cdot \sum_{q'} e_{q'} \bar{q}'_\beta \gamma_\mu R q'_\beta, & O_8 &= \frac{3}{2} \bar{d}_\alpha \gamma^\mu L b_\beta \cdot \sum_{q'} e_{q'} \bar{q}'_\beta \gamma_\mu R q'_\alpha, \\ O_9 &= \frac{3}{2} \bar{d}_\alpha \gamma^\mu L b_\alpha \cdot \sum_{q'} e_{q'} \bar{q}'_\beta \gamma_\mu L q'_\beta, & O_{10} &= \frac{3}{2} \bar{d}_\alpha \gamma^\mu L b_\beta \cdot \sum_{q'} e_{q'} \bar{q}'_\beta \gamma_\mu L q'_\alpha, \end{aligned} \quad (24)$$

where  $\alpha$  and  $\beta$  are the  $SU(3)$  color indices;  $L$  and  $R$  are the left- and right-handed projection operators with  $L = (1 - \gamma_5)$ ,  $R = (1 + \gamma_5)$ . The sum over  $q'$  runs over the quark fields that are active at the scale  $\mu = O(m_b)$ , i.e.,  $(q' \in \{u, d, s, c, b\})$ .

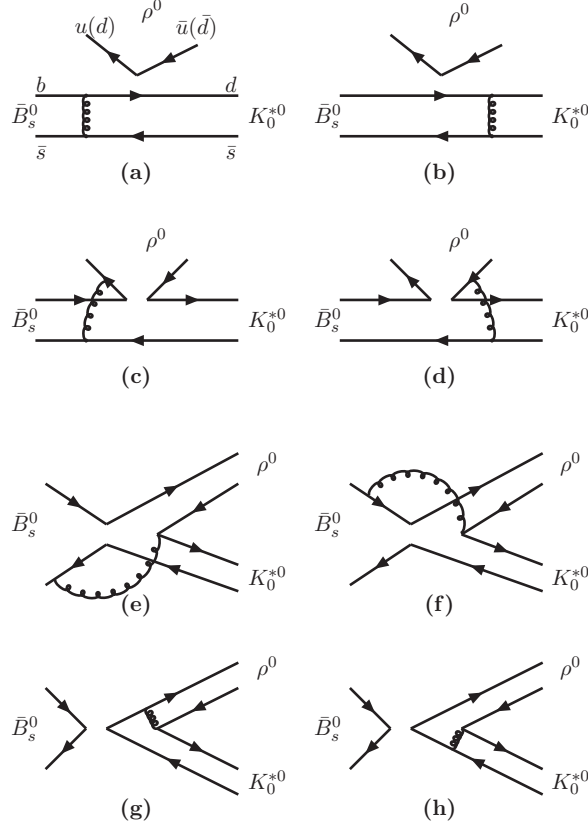


FIG. 1: Diagrams contributing to the decay  $\bar{B}_s^0 \rightarrow \rho^0 K_0^{*0}(1430)$ .

In Fig. 1, we give the leading order Feynman diagrams for the channel  $\bar{B}_s^0 \rightarrow \rho^0 K_0^{*0}(1430)$  as an example. The Feynman diagrams for the other decays are similar and not given. The analytic formulas of each considered decays are similar to those of  $B \rightarrow f_0(980)K^*$  [15] and  $B \rightarrow K_0^*(1430)\rho(\omega)$  [16]. We just need to replace some corresponding wave functions, Wilson coefficients, and parameters. Here we do not show these formulas.

Combining the contributions from different diagrams, the total decay amplitudes for these decays can be written as

$$\begin{aligned}
\sqrt{2}\mathcal{M}(K_0^{*0}\rho^0) = & \xi_u [M_{eK_0^*}C_2 + F_{eK_0^*}a_2] - \xi_t \left[ F_{eK_0^*} \left( -a_4 + \frac{1}{2}(3C_7 + C_8) + \frac{5}{3}C_9 + C_{10} \right) \right. \\
& + M_{eK_0^*} \left( -\frac{C_3}{3} + \frac{C_9}{6} + \frac{3C_{10}}{2} \right) - (M_{eK_0^*}^{P1} + M_{aK_0^*}^{P1})(C_5 - \frac{C_7}{2}) + M_{eK_0^*}^{P2} \frac{3C_8}{2} \\
& \left. - M_{aK_0^*}(C_3 - \frac{1}{2}C_9) - F_{aK_0^*}(a_4 - \frac{1}{2}a_{10}) - F_{aK_0^*}^{P2}(a_6 - \frac{1}{2}a_8) \right], \quad (25)
\end{aligned}$$

$$\begin{aligned}
\sqrt{2}\mathcal{M}(K_0^{*0}\omega) = & \xi_u [M_{eK_0^*}C_2 + F_{eK_0^*}a_2] - \xi_t \left[ F_{eK_0^*} \left( \frac{7C_3}{3} + \frac{5C_4}{3} + 2a_5 + \frac{a_7}{2} + \frac{C_9}{3} - \frac{C_{10}}{3} \right) \right. \\
& + M_{eK_0^*} \left( \frac{C_3}{3} + 2C_4 - \frac{C_9}{6} + \frac{C_{10}}{2} \right) + (M_{eK_0^*}^{P1} + M_{aK_0^*}^{P1})(C_5 - \frac{C_7}{2}) \\
& + M_{eK_0^*}^{P2} (2C_6 + \frac{C_8}{2}) + M_{aK_0^*} (C_3 - \frac{1}{2}C_9) + F_{aK_0^*} (a_4 - \frac{1}{2}a_{10}) \\
& \left. + F_{aK_0^*}^{P2} (a_6 - \frac{1}{2}a_8) \right], \tag{26}
\end{aligned}$$

$$\begin{aligned}
\mathcal{M}(K_0^{*+}\rho^-) = & \xi_u [M_{eK_0^*}C_1 + F_{eK_0^*}a_1] - \xi_t [F_{eK_0^*} (a_4 + a_{10}) + M_{eK_0^*} (C_3 + C_9) \\
& + M_{eK_0^*}^{P1} (C_5 + C_7) + M_{aK_0^*} (C_3 - \frac{1}{2}C_9) + M_{aK_0^*}^{P1} (C_5 - \frac{1}{2}C_7) \\
& + F_{aK_0^*} (a_4 - \frac{1}{2}a_{10}) + F_{aK_0^*}^{P2} (a_6 - \frac{1}{2}a_8)], \tag{27}
\end{aligned}$$

$$\begin{aligned}
\mathcal{M}(K_0^{*0}\phi) = & -\xi_t \left[ F_{e\phi}^{P2} (a_6 - \frac{a_8}{2}) + M_{e\phi} (C_3 - \frac{C_9}{2}) + (M_{e\phi}^{P1} + M_{a\phi}^{P1})(C_5 - \frac{C_7}{2}) \right. \\
& + M_{a\phi} (C_3 - \frac{1}{2}C_9) + F_{a\phi} (a_4 - \frac{1}{2}a_{10}) + F_{a\phi} (a_6 - \frac{1}{2}a_8) \\
& + F_{eK_0^*} \left( a_3 + a_5 - \frac{1}{2}a_7 - \frac{1}{2}a_7 \right) + M_{eK_0^*} (C_4 - \frac{1}{2}C_{10}) \\
& \left. + M_{eK_0^*}^{P2} (C_6 - \frac{1}{2}C_8) \right]. \tag{28}
\end{aligned}$$

The combinations of the Wilson coefficients are defined as usual [28]:

$$\begin{aligned}
a_1(\mu) &= C_2(\mu) + \frac{C_1(\mu)}{3}, \quad a_2(\mu) = C_1(\mu) + \frac{C_2(\mu)}{3}, \\
a_i(\mu) &= C_i(\mu) + \frac{C_{i+1}(\mu)}{3}, \quad i = 3, 5, 7, 9, \\
a_i(\mu) &= C_i(\mu) + \frac{C_{i-1}(\mu)}{3}, \quad i = 4, 6, 8, 10. \tag{29}
\end{aligned}$$

#### IV. NUMERICAL RESULTS AND DISCUSSIONS

We use the following input parameters in the numerical calculations [29]:

$$f_{B_s} = 230 \text{ MeV}, M_{B_s} = 5.37 \text{ GeV}, M_W = 80.41 \text{ GeV}, \tag{30}$$

$$V_{ub} = |V_{ub}|e^{-i\gamma} = 3.93 \times 10^{-3}e^{-i68^\circ}, V_{ud} = 0.974, \tag{31}$$

$$V_{td} = |V_{td}|e^{-i\beta} = 8.1 \times 10^{-3}e^{-i21.6^\circ}, V_{tb} = 1.0, \tag{32}$$

$$\alpha = 100^\circ \pm 20^\circ, \tau_{B_s} = 1.470 \times 10^{-12} \text{ s}. \tag{33}$$

Using the wave functions and the values of relevant input parameters, we find the numerical values of the corresponding form factors  $\bar{B}_s^0 \rightarrow \phi, K_0^*(1430)$  at zero momentum

transfer

$$A_0^{\bar{B}_s^0 \rightarrow \phi}(q^2 = 0) = 0.29_{-0.04-0.01}^{+0.05+0.01}, \quad (34)$$

$$F_0^{\bar{B}_s^0 \rightarrow K_0^*}(q^2 = 0) = -0.30_{-0.03-0.01-0.01}^{+0.03+0.01+0.01}, \quad \text{scenario I}, \quad (35)$$

$$F_0^{\bar{B}_s^0 \rightarrow K_0^*}(q^2 = 0) = 0.56_{-0.07-0.04-0.05}^{+0.05+0.03+0.04}, \quad \text{scenario II}, \quad (36)$$

where the uncertainties are from  $\omega_{b_s} = 0.5 \pm 0.05$  of  $B_s$  and the Gegenbauer moment  $a_{2\phi} = 0.18 \pm 0.08$  of the vector meson  $\phi$  for  $A_0^{\bar{B}_s^0 \rightarrow \phi}$ , and from the decay constant, the Gegenbauer moments  $B_1$  and  $B_3$  of the scalar meson  $K_0^*$  for  $F_0^{\bar{B}_s^0 \rightarrow K_0^*}$ . For the  $\bar{B}_s \rightarrow \phi$  transition form factor, its value is about 0.30, which is favored by many model calculations [30–32], while a large value  $A_0^{\bar{B}_s \rightarrow \phi} = 0.474$  is obtained by the light-cone sum-rule method [24]. The discrepancy can be clarified by the current LHC-b experiments. As for the form factors  $F_0^{\bar{B}_s^0 \rightarrow K_0^*}$  in two scenarios, they agree well with those given in [33].

In the  $B_s$ -rest frame, the decay rates of  $\bar{B}_s^0 \rightarrow K_0^*(1430)\rho(\omega, \phi)$  can be written as

$$\Gamma = \frac{G_F^2}{32\pi m_{B_s}} |\mathcal{M}|^2 (1 - r_{K_0^*}^2), \quad (37)$$

where  $\mathcal{M}$  is the total decay amplitude of each considered decay and  $r_{K_0^*}$  is the mass ratio, both of which have been given in Sec. III. The  $\mathcal{M}$  can be rewritten as

$$\mathcal{M} = V_{ub}V_{ud}^*T - V_{tb}V_{td}^*P = V_{ub}V_{ud}^* [1 + ze^{i(\alpha+\delta)}], \quad (38)$$

where  $\alpha$  is the Cabibbo-Kobayashi-Maskawa weak phase angle, and  $\delta$  is the relative strong phase between the tree and the penguin amplitudes, which are denoted as "T" and "P," respectively. The term  $z$  describes the ratio of penguin to tree contributions and is defined as

$$z = \left| \frac{V_{tb}V_{td}^*}{V_{ub}V_{ud}^*} \right| \left| \frac{P}{T} \right|. \quad (39)$$

From Eq.(38), it is easy to write decay amplitude  $\overline{\mathcal{M}}$  for the corresponding conjugated decay mode. So the CP-averaged branching ratio for each considered decay is defined as

$$\mathcal{B} = (|\mathcal{M}|^2 + |\overline{\mathcal{M}}|^2)/2 = |V_{ub}V_{ud}^*T|^2 [1 + 2z \cos \alpha \cos \delta + z^2]. \quad (40)$$

Using the input parameters and the wave functions as specified in this section and Sec. II, we can calculate the branching ratios of the considered modes

$$\mathcal{B}(\bar{B}_s^0 \rightarrow K_0^{*0}(1430)\phi) = (2.9_{-0.5-0.1-0.5}^{+0.6+0.2+0.6}) \times 10^{-7}, \quad \text{scenario I}, \quad (41)$$

$$\mathcal{B}(\bar{B}_s^0 \rightarrow K_0^{*0}(1430)\omega) = (8.2_{-1.6-0.1-0.6}^{+1.7+0.0+0.6}) \times 10^{-7}, \quad \text{scenario I}, \quad (42)$$

$$\mathcal{B}(\bar{B}_s^0 \rightarrow K_0^{*0}(1430)\rho^0) = (9.9_{-1.9-0.1-0.7}^{+2.0+0.0+0.7}) \times 10^{-7}, \quad \text{scenario I}, \quad (43)$$

$$\mathcal{B}(\bar{B}_s^0 \rightarrow K_0^{*+}(1430)\rho^-) = (3.4_{-0.6-0.2-0.2}^{+0.7+0.3+0.3}) \times 10^{-5}, \quad \text{scenario I}, \quad (44)$$

$$\mathcal{B}(\bar{B}_s^0 \rightarrow K_0^{*0}(1430)\phi) = (9.5_{-1.7-1.9-1.4}^{+2.5+2.8+3.1}) \times 10^{-7}, \quad \text{scenario II}, \quad (45)$$

$$\mathcal{B}(\bar{B}_s^0 \rightarrow K_0^{*0}(1430)\omega) = (8.6_{-1.8-0.5-1.5}^{+2.1+0.6+2.2}) \times 10^{-7}, \quad \text{scenario II}, \quad (46)$$

$$\mathcal{B}(\bar{B}_s^0 \rightarrow K_0^{*0}(1430)\rho^0) = (9.6_{-2.0-0.4-2.1}^{+2.2+0.4+2.0}) \times 10^{-7}, \quad \text{scenario II}, \quad (47)$$

$$\mathcal{B}(\bar{B}_s^0 \rightarrow K_0^{*+}(1430)\rho^-) = (10.8_{-2.3-1.1-1.7}^{+2.5+1.2+1.9}) \times 10^{-5}, \quad \text{scenario II}, \quad (48)$$



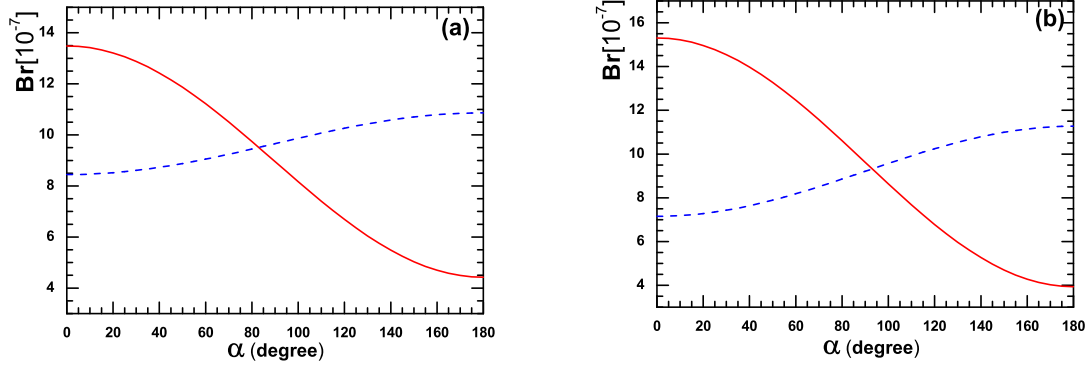


FIG. 2: The dependence of the branching ratios for  $\bar{B}_s^0 \rightarrow K_0^{*0}(1430)\omega$  (solid curve),  $\bar{B}_s^0 \rightarrow K_0^{*0}(1430)\rho^0$  (dashed curve) on the Cabibbo-Kobayashi-Maskawa angle  $\alpha$ . The left (right) panel is plotted in scenario I (II).

where the uncertainties are mainly from the decay constant, the Gegenbauer moments  $B_1$  and  $B_3$  of the scalar meson  $K_0^*$ . From the results, one can find that the branching ratios of  $\bar{B}_s^0 \rightarrow K_0^{*0}(1430)\phi, K_0^{*+}(1430)\rho^-$  in scenario II are about  $3.2 \sim 3.3$  times larger than those in scenario I. While for the decays  $\bar{B}_s^0 \rightarrow K_0^{*0}(1430)\omega(\rho^0)$ , their branching ratios for two scenarios are very close to each other, respectively. In these four decay channels, the branching ratio of  $\bar{B}_s^0 \rightarrow K_0^{*+}(1430)\rho^-$  is the largest one. This is not a surprise: one can recall that the channel  $\bar{B}_s^0 \rightarrow K_0^+\rho^-$  also receives a large branching ratio, about  $(2.45^{+1.52}_{-1.29}) \times 10^{-5}$  predicted by the QCD factorization approach [34] and about  $(1.78^{+0.78}_{-0.59}) \times 10^{-5}$  predicted by the PQCD approach [35]. Certainly, for the other three decays  $\bar{B}_s^0 \rightarrow K_0^{*0}(1430)\phi, K_0^{*0}(1430)\omega(\rho^0)$ , their branch ratios have the same order with those of the decays  $\bar{B}_s^0 \rightarrow K_0^0\phi, K_0^0\omega(\rho^0)$ , which are listed in Table I. It is easy to get the conclusion that the branching ratios of the decays  $\bar{B}_s^0 \rightarrow K_0^*(1430)V$  are not far away from those of  $\bar{B}_s^0 \rightarrow KV$ , where  $V$  represents  $\rho, \omega, \phi$ . The same conclusion is also obtained in Ref.[12]. In Table II, we list the values of the factorizable and nonfactorizable amplitudes from the emission and annihilation topology diagrams of the decays  $\bar{B}_s^0 \rightarrow K_0^{*0}(1430)\rho^0$  and  $\bar{B}_s^0 \rightarrow K_0^{*+}(1430)\rho^-$ .  $F_{e(a)K_0^*}$  and  $M_{e(a)K_0^*}$  are the  $\rho$  meson emission (annihilation) factorizable contributions and nonfactorizable contributions from penguin operators respectively. The upper label  $T$  denotes the contributions from tree operators. For the decay  $\bar{B}_s^0 \rightarrow K_0^{*0}(1430)\rho^0$ , there are not diagrams obtained by exchanging the position of  $K_0^{*0}$  and  $\rho^0$  in Fig.1, so there are not contributions from  $F_{e(a)\rho}$  and  $M_{e(a)\rho}$ . It is same for the decay  $\bar{B}_s^0 \rightarrow K_0^{*+}(1430)\rho^-$ . From Table II, one can find that because of the large Wilson coefficients  $a_1 = C_2 + C_1/3$ , the tree-dominated decay channel  $\bar{B}_s^0 \rightarrow K_0^{*+}(1430)\rho^-$  receives a large branching ratio value in both scenarios compared with  $\bar{B}_s^0 \rightarrow K_0^{*0}(1430)\rho^0$ .

The dependence of the branching ratios for the decays  $\bar{B}_s^0 \rightarrow K_0^{*0}(1430)\rho^0, K_0^{*0}(1430)\omega, K_0^{*+}(1430)\rho^-$  on the Cabibbo-Kobayashi-Maskawa angle  $\alpha$  is displayed in Fig.2 and Fig.3. The branching ratios of the  $K_0^{*0}(1430)\rho^0$  and  $K_0^{*+}(1430)\rho^-$

TABLE I: Comparing the branching ratios of  $\bar{B}_s^0 \rightarrow K_0^0 \phi, K_0^0 \omega, K_0^0 \rho^0, K_0^+ \rho^-$  predicted in [34] and those of  $\bar{B}_s^0 \rightarrow K_0^{*0}(1430) \phi, K_0^{*0}(1430) \omega, K_0^{*0}(1430) \rho^0, K_0^{*+}(1430) \rho^-$  predicted in this work in scenario I .

Mode	Br( $\times 10^{-6}$ )
$\bar{B}_s^0 \rightarrow K_0^{*0}(1430) \phi$	$0.29^{+0.06+0.02+0.06}_{-0.05-0.01-0.05}$
$\bar{B}_s^0 \rightarrow K_0^0 \phi$	$0.27^{+0.09+0.28+0.09+0.67}_{-0.08-0.14-0.06-0.18}$
$\bar{B}_s^0 \rightarrow K_0^{*0}(1430) \omega$	$0.82^{+0.17+0.00+0.06}_{-0.16-0.01-0.06}$
$\bar{B}_s^0 \rightarrow K_0^0 \omega$	$0.51^{+0.20+0.15+0.68+0.40}_{-0.18-0.11-0.23-0.25}$
$\bar{B}_s^0 \rightarrow K_0^{*0}(1430) \rho^0$	$0.99^{+0.02+0.00+0.07}_{-0.19-0.01-0.07}$
$\bar{B}_s^0 \rightarrow K_0^0 \rho^0$	$0.61^{+0.33+0.21+1.06+0.56}_{-0.26-0.15-0.38-0.36}$
$\bar{B}_s^0 \rightarrow K_0^{*+}(1430) \rho^-$	$34.0^{+0.7+0.3+0.3}_{-0.6-0.2-0.2}$
$\bar{B}_s^0 \rightarrow K_0^+ \rho^-$	$24.5^{+11.9+9.2+1.8+1.6}_{-9.7-7.8-3.0-1.6}$

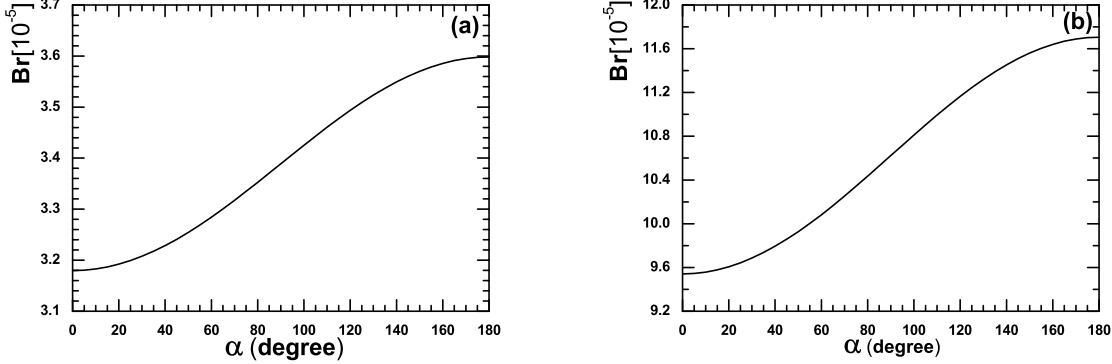


FIG. 3: The dependence of the branching ratio for  $\bar{B}_s^0 \rightarrow K_0^{*+}(1430) \rho^-$  on the Cabibbo-Kobayashi-Maskawa angle  $\alpha$ . The left (right) panel is plotted in scenario I (II).

modes increase with  $\alpha$ , while that of the  $K_0^{*0}(1430) \omega$  mode decreases with  $\alpha$ . The values of  $\cos \delta$  [shown in Eq.(40)] for the decay modes  $\bar{B}_s^0 \rightarrow K_0^{*0}(1430) \rho^0, K_0^{*+}(1430) \rho^-$  are opposite in sign with that of  $\bar{B}_s^0 \rightarrow K_0^{*0}(1430) \omega$ , and as a result the behaviors of the branching ratios with the Cabibbo-Kobayashi-Maskawa angle  $\alpha$  for the former are very different with that of the latter. We can also find that the branching ratio of the decay  $\bar{B}_s^0 \rightarrow K_0^{*+}(1430) \rho^-$  is insensitive to the variation of  $\alpha$  in scenario I. For the decay  $\bar{B}_s^0 \rightarrow K_0^{*0}(1430) \phi$ , there are only penguin operator contributions in this channel, so its branching ratio has no relation with the angle  $\alpha$  at the leading order.

Now, we turn to the evaluations of the direct CP-violating asymmetries of the considered decays in the PQCD approach. The direct CP-violating asymmetry can be defined

TABLE II: Decay amplitudes for decays  $\bar{B}_s^0 \rightarrow K_0^{*+}(1430)\rho^-, K_0^{*0}(1430)\rho^0$  ( $\times 10^{-2}\text{GeV}^3$ ).

	$F_{eK_0^*}^T$	$F_{eK_0^*}$	$M_{eK_0^*}^T$	$M_{eK_0^*}$	$M_{aK_0^*}$	$F_{aK_0^*}$
$\bar{B}_s^0 \rightarrow K_0^{*0}(1430)\rho^0$ (SI)	-22.4	4.9	$-11.7 + 8.2i$	$-0.15 + 0.24i$	$-0.14 + 0.11i$	$-4.1 - 2.9i$
$\bar{B}_s^0 \rightarrow K_0^{*+}(1430)\rho^-$ (SI)	203	-8.6	$6.5 - 5.2i$	$0.08 - 0.28i$	$0.16 - 0.09i$	$5.3 + 4.4i$
$\bar{B}_s^0 \rightarrow K_0^{*0}(1430)\rho^0$ (SII)	27.6	-7.8	$0.7 + 5.9i$	$0.36 - 0.20i$	$0.40 + 0.20i$	$3.1 + 8.1i$
$\bar{B}_s^0 \rightarrow K_0^{*+}(1430)\rho^-$ (SII)	-371	14.3	$-0.04 - 4.6i$	$0.58 + 0.41i$	$-0.58 - 0.28i$	$-4.1 - 11.5i$

as

$$\mathcal{A}_{CP}^{dir} = \frac{|\overline{\mathcal{M}}|^2 - |\mathcal{M}|^2}{|\mathcal{M}|^2 + |\overline{\mathcal{M}}|^2} = \frac{2z \sin \alpha \sin \delta}{1 + 2z \cos \alpha \cos \delta + z^2}. \quad (49)$$

Here the ratio  $z$  and the strong phase  $\delta$  are calculable in PQCD approach, so it is easy to find the numerical values of  $\mathcal{A}_{CP}^{dir}$  (in unit of  $10^{-2}$ ) by using the input parameters listed in the previous for the considered decays in two scenarios:

$$\mathcal{A}_{CP}^{dir}(\bar{B}_s^0 \rightarrow K_0^{*0}(1430)\omega) = -24.1_{-0.0-2.5-0.2}^{+0.0+2.7+0.6}, \text{ scenario I}, \quad (50)$$

$$\mathcal{A}_{CP}^{dir}(\bar{B}_s^0 \rightarrow K_0^{*0}(1430)\rho^0) = 26.6_{-0.0-2.5-0.5}^{+0.0+2.5+0.3}, \text{ scenario I}, \quad (51)$$

$$\mathcal{A}_{CP}^{dir}(\bar{B}_s^0 \rightarrow K_0^{*+}(1430)\rho^-) = 7.7_{-0.0-0.3-0.2}^{+0.0+0.2+0.2}, \text{ scenario I}, \quad (52)$$

$$\mathcal{A}_{CP}^{dir}(\bar{B}_s^0 \rightarrow K_0^{*0}(1430)\omega) = -86.7_{-0.1-5.3-2.8}^{+0.1+7.1+1.3}, \text{ scenario II}, \quad (53)$$

$$\mathcal{A}_{CP}^{dir}(\bar{B}_s^0 \rightarrow K_0^{*0}(1430)\rho^0) = 84.5_{-0.1-6.3-3.8}^{+0.1+4.9+1.0}, \text{ scenario II}, \quad (54)$$

$$\mathcal{A}_{CP}^{dir}(\bar{B}_s^0 \rightarrow K_0^{*+}(1430)\rho^-) = 12.6_{-0.0-0.2-0.6}^{+0.0+0.2+0.8}, \text{ scenario II}, \quad (55)$$

where the uncertainties are mainly from the decay constant, the Gegenbauer moments  $B_1$  and  $B_3$  of the scalar meson  $K_0^*$ . Compared with the values of the branching ratios, we can find that if the direct CP-violating asymmetries are sensitive to some parameters, while the branching ratios are insensitive to them, for example, the decay constant of  $K_0^*$ . For the decays  $\bar{B}_s^0 \rightarrow K_0^{*0}(1430)\omega, K_0^{*0}(1430)\rho^0$ , their direct CP-violating asymmetries in scenario II are more than 3 times than those in scenario I. In both scenarios, the direct CP-violating asymmetries of these two decay channels are close to each other in size, while they are opposite in sign. The reason for this is the following. The mesons  $\rho^0, \omega$  have very similar mass, decay constant, and distribution amplitude, only the opposite sign of  $d\bar{d}$  in their quark components, and the difference will appear in penguin operators. From our numerical results, we can find that the contributions from tree operators for these two channels (denoted as  $T_{K_0^{*0}\rho^0}$  and  $T_{K_0^{*0}\omega}$ ) are really very close, and those from penguin operators for these two channels (denoted as  $P_{K_0^{*0}\rho^0}$  and  $P_{K_0^{*0}\omega}$ ) are opposite in sign. Furthermore, the real parts of  $P_{K_0^{*0}\rho^0}$  and  $P_{K_0^{*0}\omega}$  in each scenario have large differences in size.

$$T_{K_0^{*0}\rho^0} = (-34.1 + i8.2) \times 10^{-2}, P_{K_0^{*0}\rho^0} = (0.49 - i2.5) \times 10^{-2}, \quad (56)$$

$$T_{K_0^{*0}\omega} = (-31.8 + i7.6) \times 10^{-2}, P_{K_0^{*0}\omega} = (-3.7 + i2.8) \times 10^{-2}, \text{ scenario I}, \quad (57)$$

$$T_{K_0^{*0}\rho^0} = (28.3 + i5.9) \times 10^{-2}, P_{K_0^{*0}\rho^0} = (-3.9 + i8.1) \times 10^{-2}, \quad (58)$$

$$T_{K_0^{*0}\omega} = (26.4 + i5.5) \times 10^{-2}, P_{K_0^{*0}\omega} = (8.1 - i7.2) \times 10^{-2}, \text{ scenario II}. \quad (59)$$

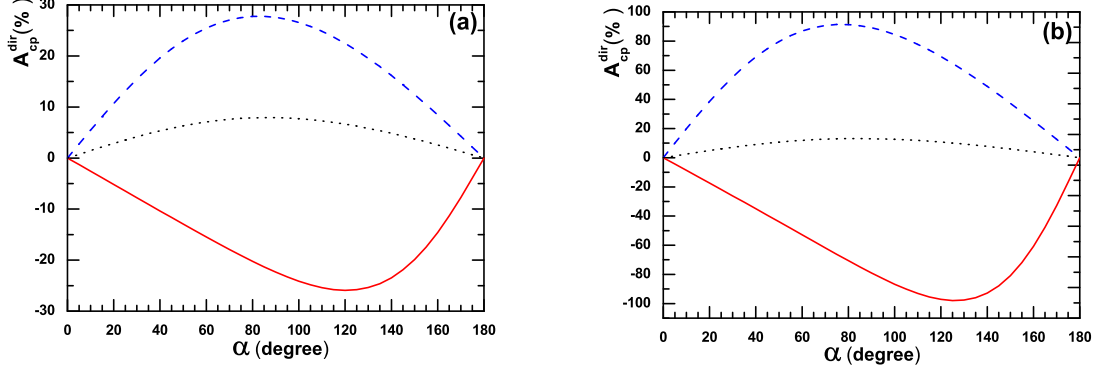


FIG. 4: The dependence of the direct CP asymmetries for  $\bar{B}_s^0 \rightarrow K_0^{*0}(1430)\omega$  (solid curve),  $\bar{B}_s^0 \rightarrow K_0^{*+}(1430)\rho^-$  (dotted curve),  $\bar{B}_s^0 \rightarrow K_0^{*0}(1430)\rho^0$  (dashed curve) on the Cabibbo-Kobayashi-Maskawa angle  $\alpha$ . The left (right) panel is plotted in scenario I (II)

These values can explain why the two channels have similar CP-violating asymmetry in size (certainly, their branching ratios are also similar for the same reason). Using the upper results, we can calculate  $\sin \delta$  [shown in Eq.(49)] in two scenarios:

$$\sin \delta_{K_0^{*0}\rho^0} = 0.91, \sin \delta_{K_0^{*0}\omega} = -0.40, \text{ scenario I,} \quad (60)$$

$$\sin \delta_{K_0^{*0}\rho^0} = 0.97, \sin \delta_{K_0^{*0}\omega} = -0.80, \text{ scenario II.} \quad (61)$$

These values can explain why the CP-violating asymmetries of these two decays have opposite signs.

The direct CP-violating asymmetry of  $\bar{B}_s^0 \rightarrow K_0^{*+}(1430)\rho^-$  is the smallest in these decays, about 10%, but its branching ratio is the largest one, about  $3.4 \times 10^{-5}$  in scenario I, even at the order of  $10^{-4}$  in scenario II. So this channel might be easily measured at LHC-b experiments. From Fig.4(a) and 4(b), one can see that though the direct CP asymmetry values for each decay in two scenarios are very different in size, they have similar trends depending on the Cabibbo-Kobayashi-Maskawa angle  $\alpha$ . As for the decay  $\bar{B}_s^0 \rightarrow K_0^{*0}(1430)\phi$ , there is no tree contribution at the leading order, so the direct CP-violating asymmetry is naturally zero.

## V. CONCLUSION

In this paper, we calculate the branching ratios and the CP-violating asymmetries of decays  $\bar{B}_s^0 \rightarrow K_0^{*}(1430)\rho(\omega, \phi)$  in the PQCD factorization approach. Using the decay constants and light-cone distribution amplitudes derived from QCD sum-rule method, we find that

- We predict the form factor  $A_0^{\bar{B}_s^0 \rightarrow \phi}(q^2 = 0) = 0.29_{-0.04}^{+0.05+0.01}$  for  $\omega_{b_s} = 0.5 \pm 0.05$  and the Gegenbauer moment  $a_{2\phi} = 0.18 \pm 0.08$ , which agrees well with the values

as calculated by many approaches and disagrees with the value  $A_0^{\bar{B}_s^0 \rightarrow \phi} = 0.474$  obtained by the light-cone sum-rule method. The discrepancy can be clarified by the LHC-b experiments. The form factors of  $\bar{B}_s^0 \rightarrow K_0^*(q^2 = 0)$  in two scenarios are given as

$$F_0^{\bar{B}_s^0 \rightarrow K_0^*}(q^2 = 0) = -0.30_{-0.03-0.01-0.01}^{+0.03+0.01+0.01}, \quad \text{scenario I}, \quad (62)$$

$$F_0^{\bar{B}_s^0 \rightarrow K_0^*}(q^2 = 0) = 0.56_{-0.07-0.04-0.05}^{+0.05+0.03+0.04}, \quad \text{scenario II}, \quad (63)$$

where the uncertainties are from the decay constant, the Gegenbauer moments  $B_1$  and  $B_3$  of the scalar meson  $K_0^*$ .

- Because of the large Wilson coefficients  $a_1 = C_2 + C_1/3$ , the branching ratios of  $\bar{B}_s^0 \rightarrow K_0^{*+}(1430)\rho^-$  are much larger than those of the other three decays in both scenarios and arrive at a few times  $10^{-5}$  in scenario I, even at the  $10^{-4}$  order in scenario II, while its direct CP-violating asymmetry is the smallest one, around 10%. The values for this channel might be measured by the current LHC-b experiments.
- For the decays  $\bar{B}_s^0 \rightarrow K_0^{*0}(1430)\omega, K_0^{*0}(1430)\rho^0$ , their direct CP-violating asymmetries are large, but it might be difficult to measure them, because their branching ratios are small and less than (or near)  $10^{-6}$  in both scenarios.
- The values of  $\cos \delta$  for the decays  $\bar{B}_s^0 \rightarrow K_0^{*0}(1430)\rho^0, K_0^{*+}(1430)\rho^-$  are opposite in sign with that for  $\bar{B}_s^0 \rightarrow K_0^{*0}(1430)\omega$ ; as a result, the behaviors of the branching ratios of the former with Cabibbo-Kobayashi-Maskawa angle  $\alpha$  are very different with that of the latter. Because the values of  $\sin \delta$  are opposite in sign, their direct CP-violating asymmetries of the former have an opposite sign with that of the latter. Here  $\delta$  is the relative strong phase angle between the tree and the penguin amplitudes.
- Because the mesons  $\rho^0, \omega$  have very similar mass, decay constant, distribution amplitude, only opposite sign of  $d\bar{d}$  in their quark components, and this difference only appears in the penguin operators; so these two tree document decays  $\bar{B}_s^0 \rightarrow K_0^{*0}(1430)\rho^0$  and  $\bar{B}_s^0 \rightarrow K_0^{*0}(1430)\omega$  should have similar branching ratios and CP-violating asymmetries.
- As for the decay  $\bar{B}_0^s \rightarrow K_0^{*0}(1430)\phi$ , though there exist large differences between the two scenarios, the predicted branching ratios are small and a few times  $10^{-7}$  in both scenarios. There is no tree contribution at the leading order, so the direct CP-violating asymmetry is naturally zero.

## Acknowledgment

This work is partly supported by the National Natural Science Foundation of China under Grant No. 11047158, and by Foundation of Henan University of Technology under

Grant No.150374. The author would like to thank Cai-Dian Lü for helpful discussions.

- 
- [1] N. A. Tornqvist, Phys. Rev. Lett. **49**, 624 (1982).
  - [2] G.L. Jaffe, Phys. Rev. D **15**, 267 (1977); Erratum-ibid. Phys. Rev. D **15** 281 (1977); A. L. Kataev, Phys. Atom. Nucl. **68**, 567 (2005), Yad. Fiz. **68**, 597 (2005); A. Vijande, A. Valcarce, F. Fernandez and B. Silvestre-Brac, Phys. Rev. D **72**, 034025 (2005).
  - [3] J. Weinstein , N. Isgur , Phys. Rev. Lett. **48**, 659 (1982); Phys. Rev. D **27**, 588 (1983); **41**, 2236 (1990); M. P. Locher, *et al.*, Eur. Phys. J. C **4**, 317 (1998).
  - [4] V. Baru, *et al.*, Phys. Lett. B **586**, 53 (2004).
  - [5] L. Celenza, *et al.*, Phys. Rev. C **61** (2000) 035201.
  - [6] M. Strohmeier-Presicek, *et al.*, Phys. Rev. D **60** 054010 (1999).
  - [7] F. E. Close, A. Kirk, Phys. Lett. B **483** 345 (2000).
  - [8] A. K. Giri , B. Mawlong, R. Mohanta Phys. Rev. D **74**, 114001 (2006).
  - [9] H. Y. Cheng, K. C. Yang Phys. Rev. D **71**, 054020 (2005).
  - [10] H. Y. Cheng , C. K. Chua , K. C. Yang Phys. Rev. D **73**, 014017 (2006).
  - [11] H. Y. Cheng, C. K. Chua and K. C. Yang, Phys. Rev. D **77**, 014034 (2008).
  - [12] Z. Q. Zhang and Z.J. Xiao, Chin. Phys. C **33**(07), 508 (2009).
  - [13] Z. Q. Zhang and Z.J. Xiao, Chin. Phys. C **34**(05), 528 (2010).
  - [14] Z. Q. Zhang, J. Phys. G **37**, 085012 (2010).
  - [15] Z. Q. Zhang, J.D. Zhang, Eur. Phys. J. C **67**, 163 (2010).
  - [16] Z. Q. Zhang, Phys. Rev. D **82**, 034036 (2010).
  - [17] N. Brambilla, *et al.*, (Quarkonium Working Group), CERN-2005-005, hep-ph/0412158; M. P. Altarelli and F. Teubert, Int. J. Mod.Phys. A **23**, 5117 (2008).
  - [18] M. Artuso, *et al.*, "B, D and K decays", Report of Working Group 2 of the CERN workshop on Flavor in the Era of the LHC, Eur. Phys. J. C **57**, 309 (2008).
  - [19] A. G. Grozin and M. Neubert, Phys. Rev. D **55**, 272 (1977); M. Beneke and T. Feldmann, Nucl. Phys.B **592**, 3 (2001).
  - [20] H. Kawamura, *et al.*, Phys.Lett.B **523**, 111 (2001); Mod. Phys. Lett. A **18**, 799 (2003).
  - [21] C. D. Lu, M. Z. Yang, Eur.Phys.J.C **28**, 515 (2003).
  - [22] Particle Data Group, W. M. Yao, *et al.*, J. Phys. G **33**, 1 (2006).
  - [23] P. Ball, G. W. Jones and R. Zwicky, Phys. Rev. D **75**, 054004 (2007).
  - [24] P. Ball and R. Zwicky, Phys. Rev. D **71**, 014029 (2005); P. Ball and R. Zwicky, JHEP **0604**, 046 (2006); P. Ball and G. W. Jones, JHEP bf0703, 069 (2007).
  - [25] H. N. Li, Phys. Rev. D **66**, 094010 (2002).
  - [26] H.N. Li and B. Tseng, Phys. Rev. D **57**, 443 (1998).
  - [27] G. Buchalla , A. J. Buras , M. E. Lautenbacher, Rev. Mod. Phys. **68**, 1125 (1996).
  - [28] Z. J. Xiao, Z. Q. Zhang, X. Liu, L. B. Guo, Phys. Rev. D **78**, 114001 (2008).
  - [29] Particle Data Group, C. Amsler, *et al.*, Phys. Lett. B **667**, 1 (2008);
  - [30] Y. L. Wu, M. Zhong and Y. B. Zuo, Int. J. Mod. Phys. A **21**, 6125 (2006).
  - [31] C. D. Lu, W. Wang and Z. T. Wei, Phys. Rev. D **76**, 014013 (2007).
  - [32] H. Y. Cheng, C. K. Chua, and C. W. Hwang, Phys. Rev. D **69**, 074025 (2004).
  - [33] R. H. Li, *et al.*, Phys. Rev. D **79**, 014013, (2009).
  - [34] M. Beneke, M. Neubert, Nucl. Phys.B **675**, 333 (2001).

[35] A. Ali, *et al.*, Phys. Rev. D **76**, 074018 (2007).